DOI: 10.3901/CJME.2016.0125.013, available online at www.springerlink.com; www.cjmenet.com

Influence of Strut Cross-section of Stents on Local Hemodynamics in Stented Arteries

JIANG Yongfei, ZHANG Jun, and ZHAO Wanhua*

State Key Laboratory for Manufacturing System Engineering, Xi'an Jiaotong University, Xi'an 710054, China

Received February 4, 2015; revised December 1, 2015; accepted January 25, 2016

Abstract: Stenting is a very effective treatment for stenotic vascular diseases, but vascular geometries altered by stent implantation may lead to flow disturbances which play an important role in the initiation and progression of restenosis, especially in the near wall in stented arterial regions. So stent designs have become one of the indispensable factors needed to be considered for reducing the flow disturbances. In this paper, the structural designs of strut cross-section are considered as an aspect of stent designs to be studied in details. Six virtual stents with different strut cross-section are designed for deployments in the same ideal arterial model. Computational fluid dynamics (CFD) methods are performed to study how the shape and the aspect ratio (AR) of strut cross-section modified the local hemodynamics in the stented segments. The results indicate that stents with different strut cross-sections have different influence on the hemodynamics. Stents with streamlined cross-sectional struts for circular arc or elliptical arc can significantly enhance wall shear stress (WSS) in the stented segments, and reduce the flow disturbances around stent struts. The performances of stents with streamlined cross-sectional struts are better than that of stents with non-streamlined cross-sectional struts for rectangle. The results also show that stents with a larger AR cross-section are more conductive to improve the blood flow. The present study provides an understanding of the flow physics in the vicinity of stent struts and indicates that the shape and AR of strut cross-section ought to be considered as important factors to minimize flow disturbance in stent designs.

Keywords: stent, restenosis, wall shear stress, hemodynamics, computational fluid dynamics

1 Introduction

A narrowed arterial lumen or arterial stenosis can limit distal blood flow and result in downstream tissue death from inadequate perfusion[1]. Many stents have been used successfully to treat stenosis vascular diseases in recent years. Except that the primary function of a stent is to provide scaffolding to hold the arterial lumen open and preserve an adequate cylindrical lumen for blood flow[1], it has some advantages, such as micro-traumatic characteristics, short-time hospital stays and high efficiency compared to bypass grafting and balloon angioplasty. However, there are still some problems such as thrombosis and restenosis after stenting.

In order to resolve these problems, much research has been carried out on the performance of stents after stent implantation from stent structural designs. But except for some studies about the mechanical supporting properties of stents[2–3], hemodynamic changes near wall induced by stents are often studies and considered to be related to the initiation and development of restenosis. Various fluid dynamics studies[4–5] demonstrate that low mean wall shear stress (WSS), oscillating WSS, and high particle residence times induced by stents easily occur in specific locations for intimal thickening in restenosis. Some animal and in vitro experimental studies[6–10] suggest that stent design is an important factor influencing the restenosis rate. Clinical reports[11–13] also consider that stent design (such as spacing, height and number of struts) can influence the low and high WSS distributions and result in restenosis. It is clear that stent design alters flow behaviors near the stented wall, which results in restenosis. Therefore, the evaluation of hemodynamics caused by stents is important to optimize stent design. The computational fluid dynamics(CFD) method has been used to study complex flow behaviors because it can provide detailed information about flow behaviors near struts in stented arteries[14–18]. Influence of some stent design parameters on hemodynamics has also been studied with the CFD method[19–20]. Among these design parameters of stents, strut cross-section is also a key part needed to be studied. While early stent designs mainly concentrate in wire coil stents (round cross-sectional struts) and slotted tubes stents (rectangular cross-sectional struts)[21], which always produce disturbed flow around struts. Furthermore, some studies[22–23] analyze the influence of stents with different cross-sectional shapes, different strut height and same strut width on hemodynamics and propose that changing stent strut profile to a more streamlined shape and decreasing the strut height can improve the hemodynamics for clinical stenting success with two-dimensional flow studies. Therefore,

* Corresponding author. E-mail: whzhao@mail.xjtu.edu.cn
Supported by National Natural Science Foundation of China (Grant No. 5775179)

based on the previous studies, keeping strut height constant, three-dimensional stent models with different shapes and aspect ratio (AR, the ratio of width to height) of strut cross-section are established for further research about the influence of strut cross-section on hemodynamics near the stented wall with the CFD method. Varying the strut cross-sectional parameters and keeping the same boundary conditions, the hemodynamics of different models after stent implantation are compared to present a proper technical solution for improving stent performances.

2 Flow Models and Numerical Methods

2.1 Stent geometry and physical models

The coronary artery is assumed to be a straight single-layer cylindrical tube with an internal diameter of 3 mm and the stent-to-artery ratio is 1:1. It is also assumed that stent models have similar structures and different strut cross-sectional shapes, such as rectangle, circular arc, and elliptical arc. Considering the calculation time, we only model four supports of stents in the axial direction and six sinusoidal parts of each support in the circumferential direction. Also, three connectors of stents in the circumferential direction are considered in all stent models to guarantee the mechanical flexibility of stents. Stent structure and strut cross-sectional shapes are depicted in Figs. 1(a) and 1(b). The strut height (h) and strut width (w) of six models are listed in Table 1. Moreover, additional lengths are added to the proximal and distal regions of stented segment for a fully developed flow, so the physical model is shown in Fig. 1(c) with a total length of 79 mm.

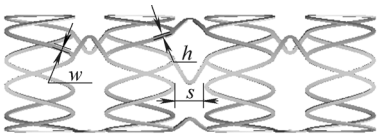

(a) Stent geometric structrue

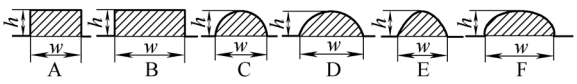

(b) Cross-sectional geometric shapes of the six stent models

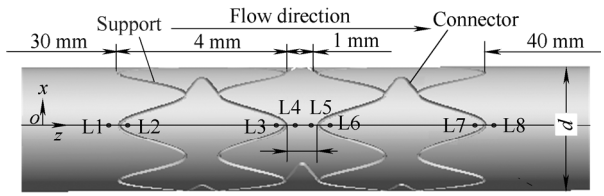

(c) Flow physical model used in the simulations

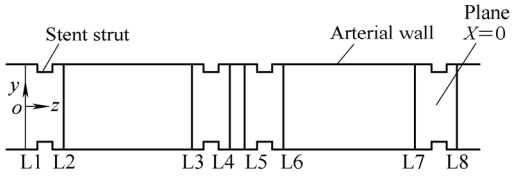

(d) Two-dimensional schematic in Plane $X=0$

Fig. 1. Stent geometric structure and flow physical model

Table 1. Parameters of six stent models

Model	Cross-sectional shapes	Strut height h/mm	Strut width w/mm
A	Rectangle	0.05	0.10
B	Rectangle	0.05	0.14
C	Circular arc	0.05	0.10
D	Circular arc	0.05	0.14
E	Elliptical arc	0.05	0.10
F	Elliptical arc	0.05	0.14

2.2 Governing equations and boundary conditions

The governing equations of mass conservation and Navier-Stokes equations are as follows:

$$\nabla \cdot \boldsymbol{V} = 0, \tag{1}$$

$$\rho \frac{\mathrm{d}\boldsymbol{V}}{\mathrm{d}t} = -\nabla \boldsymbol{p} + \mu \nabla^2 \boldsymbol{V}, \tag{2}$$

where $\boldsymbol{V}$ and $\boldsymbol{P}$ represent the blood flow velocity vector and pressure, ρ is the density of 1060 kg/m^3 and μ is the viscosity of 3.5×10^{-3} kg/m • s[24].

Blood is assumed to be an incompressible, homogeneous and Newtonian fluid[25]. The arterial wall is assumed to be rigid. All the simulations are performed with no-slip (zero-velocity) conditions between stents and artery walls and zero pressure at the outlet[25] which are expressed as Eqs. (3)–(4):

$$\boldsymbol{v}_{\mathrm{wall}} = 0, \tag{3}$$

$$\boldsymbol{p}_{\mathrm{outlet}} = 0. \tag{4}$$

Numerical simulations are conducted to elucidate the influence of strut cross-section on hemodynamics under both steady flow and pulsatile flow conditions. The purpose of steady flow is to investigate quantitatively the influence of different strut cross-sections on hemodynamics. A pulsatile flow is conducted to compare the differences of hemodynamics between steady and pulsatile flow. Given the computational time, the flow field of stents with same AR and different cross-sectional shapes (Model A, C and E) are studied under pulsatile flow.

Under steady flow conditions, the inlet velocity (v_{inlet}) is assumed to be a uniform inflow velocity profile with a value of 0.2 m/s which corresponds to the Reynolds number of 182. Similarly, under pulsatile flow conditions, a pulsatile waveform of the inlet velocity is used as inlet boundary conditions for blood flow (Fig. 2), which is based on the waveform taken from Ref. [26]. Under this flow condition, the maximum and minimum Reynolds number is 330 and 114, respectively which correspond to the largest and the lowest inlet velocity of 0.36 m/s and 0.125 m/s. So, the blood flow in arterial vessels can be considered to be laminar in all simulations. In Fig. 2, Dimensionless time t/T is scaled by the cardiac cycle period, T=0.735 s.

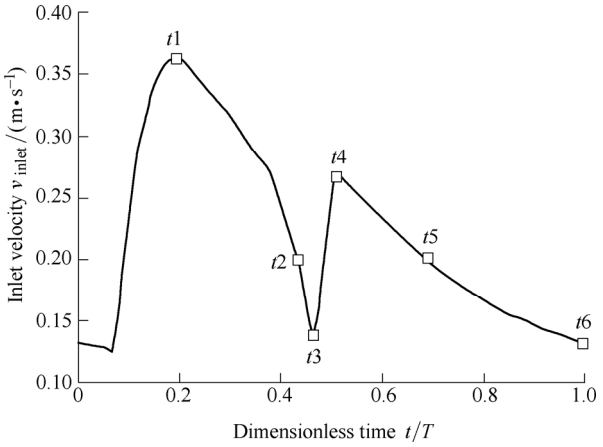

Fig. 2.　Pulsatile waveform of the inlet velocity for blood flow

2.3　Grid system and numerical methods

The physical models were imported into Gambit 2.3 (ANSYS, Inc.) to generate the computational grids for fluid domains. A mixed grid with tetrahedral elements is used to mesh the stented segments, while a cooper grid method is used to mesh the inlet and outlet segments for all models. Grid density near the stented wall is larger than elsewhere to gain more accurate WSS. The size-function in Gambit is used to mesh the stented regions (Fig. 3). Then the parameters in size-function are modified to get more refined grids for a grid-sensitivity analysis. By comparing the two adjacent simulation results, grid-independency is demonstrated until the relative difference of simulation results is less than 5% for assuring the simulation accuracy. Eventually, the number of grid elements varies from 893 670 to 2 023 927 depending on different stent geometries.

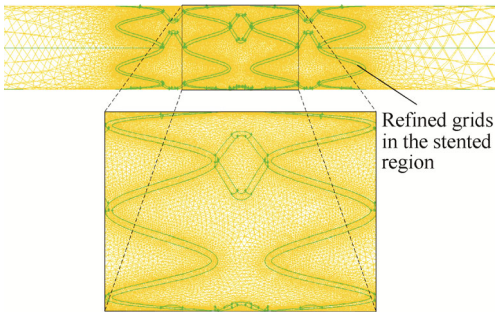

Fig. 3.　Computational grids of the physical models after stent implantation

The finite volume method is used to solve mass conservation equations and Navier-Stokes equations. A three-dimensional single-precision, segregated and laminar solver is used with second-order windward scheme to discretize these differential equations. During the solution, under-relaxation factors are set as 0.3 for pressure, 1 for density, 0.7 for momentum. Standard discretization is used for pressure with a SIMPLE algorithm under pressure-velocity coupling. Convergence criterion for mass and momentum residuals is set as 1×10^{-4}. In addition, for the time step-independence, we use 0.002 5 s as a time step size and the number of time steps is 294 per pulse cycle under the pulsatile conditions because the study results of DWYER, et al[27] found that 240 time steps per pulse cycle could give very good results with high resolution. The transient inlet velocity waveforms for the cardiac cycle are programmed into the Fluent code as UDF profile files. The simulation is computed continuously for four cardiac cycles and show that cyclic independence is achieved at the 4th cardiac cycle. So data information of some critical time points (see Fig. 2) in the 4th pulse cycle is used to analyze the hemodynamics.

3　Simulation Results

3.1　Influence of strut cross-section on flow velocity

For the physical models, the flow patterns are laminar in whole flow domains. Before encountering stents, blood flow has been to be a fully developed flow and the flow velocity profiles are almost completely similar just like parabolic curve. Then blood flow passes through the stented segments, the flow velocity profiles begin to change. In order to illustrate the flow velocity changes in stented arteries, we select eight lines (L1–L8) in Plane X=0 as shown in Figs. 1(c) and 1(d). These lines are distributed before and after stent strut with a same distance deviated from adjacent struts. The velocity profiles in the lines of L1–L8 for six physical models are depicted in Fig. 4.

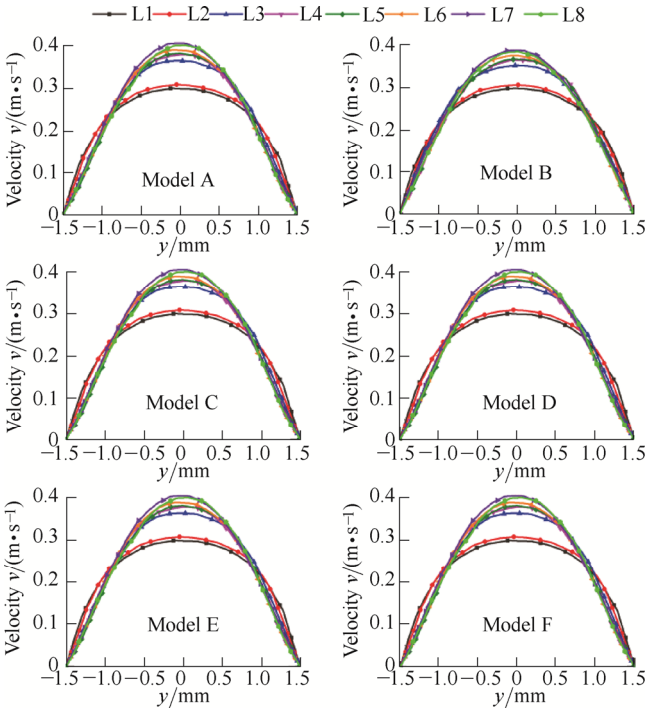

Fig. 4.　Velocity profiles in the lines of L1–L8 for six physical models after stent implantation

As a whole, stent implantations greatly improve the flow boundary conditions and the velocity profiles change gradually along the blood flow directions after encountering the stent struts. In the first line L1, the velocity changes are quite similar for all models. After

passing the first strut, the velocity distributions still maintain consistency in line L2, but the velocity values near wall decreased from L1 to L2. While from L3 to L8, except for the differences of velocity values in each line between these models, the velocity distributions are almost similar for all models. Moreover, in order to look for the differences in detail among these models, the line L5 of the stented segments for six models is selected to quantitatively analyze the differences of the velocity distributions for different cross-sections as shown in Fig. 5.

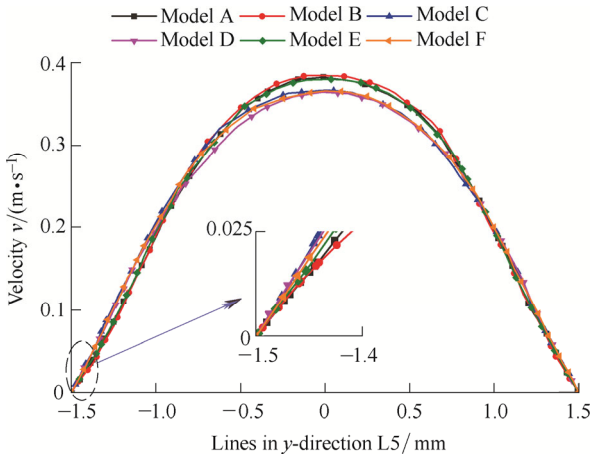

Fig. 5. Influence of strut cross-sectional shapes of stents on blood flow velocity in line L5 for six models

From overall view shown in Fig. 5, there are differences between the velocity values of these models, especially in the regions near wall. And the maximum values of the velocity appear in the center of stented arteries. The velocity variation near wall in stented segment was as follows: Model D>C>F>E>B>A. Obviously, the velocity near wall changed faster for stents with a larger AR in case of stents with same cross-sections. Moreover, the percentage of the velocity variation near wall of Model A, C and E with smaller AR decreased 4.7%, 3.7% and 13% separately compared with the corresponding Model B, D and F. Simultaneously, the influence of strut cross-sectional shapes on flow velocity near wall was also significant and compared as follows: stents with circular arc cross-section>stents with elliptical arc cross-section>stents with rectangular cross-section.

The changing trends of the velocity along flow directions were consistent for six models as shown in Fig. 4. In order to describe the velocity changes for each model, the velocity distributions of L1–L8 for the physical model D were selected and shown in Fig. 6. After blood flow passed line L2, the velocity curves began to show differences, and the velocity values near wall were getting smaller until reaching line L7. After passing the last strut near line L7, the flow velocity of L8 near wall began to increase. The comparison of the velocity values near wall for these lines was as follows: L7<L8<L6<L5<L4<L3<L2<L1 for all models. The velocity began to change quickly (from L2 to L3) before encountering the second strut, then slowed down. When passing the last strut, the flow velocity began to decrease until reaching a steady flow state.

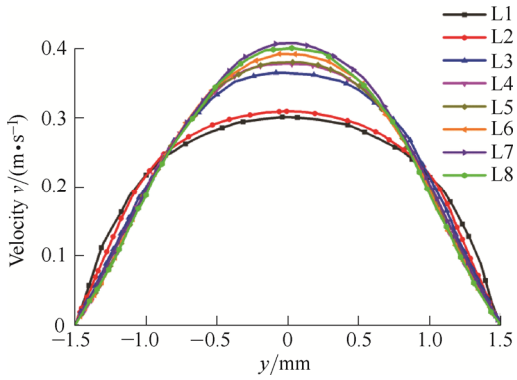

Fig. 6. Influence of strut cross-section of stents on blood flow velocity in lines of L1–L8 for the physical model D

3.2 Influence of strut cross-section on WSS

The WSS distributions were plotted in Fig. 7 for six physical models. The stent geometry had a dramatic influence on WSS from the whole distributions of all models. There were some differences for the WSS distributions among these models. After stent implantation, the highest WSS mainly occurred on the strut surface while the lowest WSS occurred in the regions around struts. Also, WSS generally increased from the regions adjacent to struts to the mesh center regions in every strut mesh (Fig. 7). But the WSS values of every strut decreased modestly with subsequent strut for six models along blood flow directions. Regions of low-WSS were mainly observed before and after each strut. The areas of low-WSS in the later strut mesh were larger than that in the former strut mesh along flow directions. The hemodynamic influence of stent strut on upstream was lower than that on downstream. Furthermore, low-WSS was prone to appear in the regions of small strut spacing, especially in these regions of peak-to-peak including connect-struts.

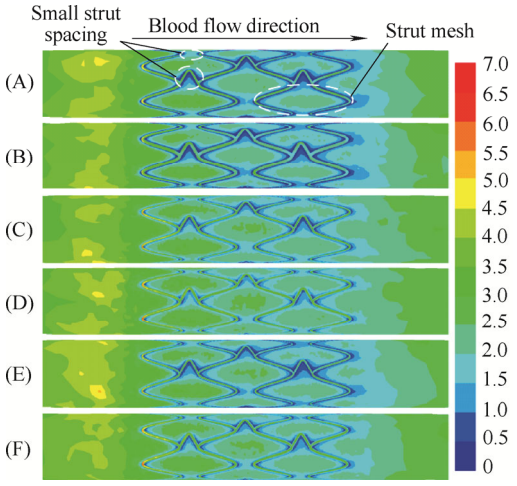

Fig. 7. Influence of strut cross-section of stents on WSS in stented sections for six models (units: Pa)

Fig. 8 shows the comparisons of WSS distributions on

the arterial wall of Plane X=0 in stented segments. It can clearly observe the differences of WSS distributions derived from stents with different cross-section and the largest WSS appear on the strut surfaces.

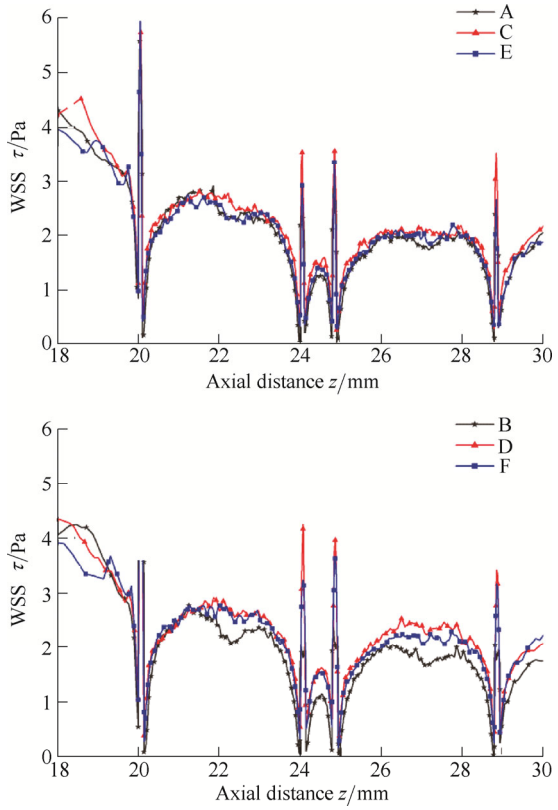

Fig. 8. Distributions of WSS at the stented wall for models with different strut cross-sectional shapes

Some previous studies[28–30] on blood flow and WSS indicated that low or oscillating WSS generated by stent implantation is easy to contribute to neointima hyperplasia, especially for the WSS value of less than 0.5 Pa. So 0.5 Pa was assumed as a critical WSS value to consider the regions prone to restenosis in this study. The data related to WSS were listed in Table 2. The average WSS ($\overline{\tau}_w$) in each model was calculated by the following equation:

$$\overline{\tau}_w = \frac{1}{A}\int_s \tau_w \mathrm{d}A, \tag{5}$$

where A was the whole luminal surface of each model, and τ_w denotes WSS.

Table 2. Comparison of main results for different models

Model	The largest value of WSS τ_{max}/Pa	Area percentage of WSS <0.5Pa p_{area}/%	Average WSS $\overline{\tau}$ /Pa
A	5.69	5.53	2.813
B	5.96	5.34	2.810
C	6.44	0.30	2.856
D	6.84	0.13	2.872
E	6.76	0.98	2.834
F	6.69	0.25	2.882

The values of average WSS for six models are above the physiological level (1–2 Pa • s) in a healthy arterial vessel[31–32], which indicates that stent implantation can improve the flow field conditions. Table 2 also shows the largest value of WSS and the vessel area percentage subjected to low-WSS on the entire fluid domain. It can be noted that the comparison of strut influence on low-WSS areas is as follows: Model A>B>E>C>F>D. For stents with the same strut height, the area percentages of low-WSS (<0.5 Pa) for struts with streamlined shapes (Models C, D, E and F) are significantly lower than that for struts with non-streamlined shapes (Models A and B). Meanwhile, it is clear that the area percentages of low-WSS for models with a larger AR are relatively low only when stents have similar cross-sectional shape. And the area percentages of low-WSS for Models B, D, and F with larger AR are respectively reduced by 3.4%, 56.7% and 74.5% when compared with Model A, C, and E correspondingly.

Especially, it is benefit to greatly improve the hemodynamics by increasing the AR of stents with streamlined cross-section. Moreover, for stents with a same AR, the influence of non-streamlined stents on hemodynamics is obviously larger than that of streamlined stents. The area percentage of low-WSS for Model A is reduced by 94.6% and 82.3%, respectively when compared with Model C and Model E. The area percentage of low-WSS for Model B is reduced by 97.6% and 95.3%, respectively when compared with Model D and Model F. Obviously, the non-streamlined stents for Model A and B with rectangular cross-section are easiest to produce low-WSS regions among these models. Therefore, stents with streamlined cross-sections for circular arc or elliptical arc and the strut cross-section with a larger AR (B>A, D>C, F>E) can remarkably improve the flow performance of stents.

3.3 Pulsatility on hemodynamics for different strut cross-sectional shape

The pulsatile simulations were conducted for three models which have different shapes and same dimensions in width and height for strut cross-section. The line L3 which positioned in stented segments and six time points showed in Fig. 2 were selected to illustrate the velocity variations with flow time (Fig. 9). For all models, the velocity distributions varied with the inlet velocity.

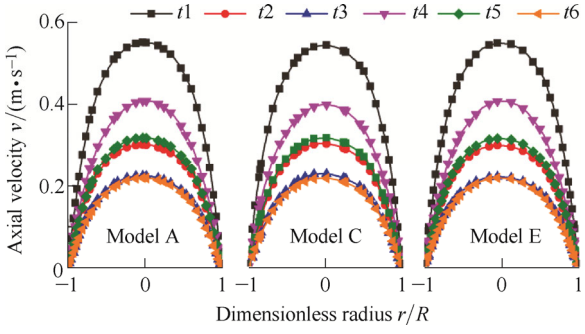

Fig. 9. Velocity distributions of line 3 for six selected time points for three models

Temporal WSS distributions in stented segments are shown in Fig. 10. The WSS magnitude at different time is significantly different due to the changes of the inlet velocity. The WSS distributions also vary with struts for different cross-sections. WSS generated by the stent with rectangular cross-section are much lower than stents with other cross-sections.

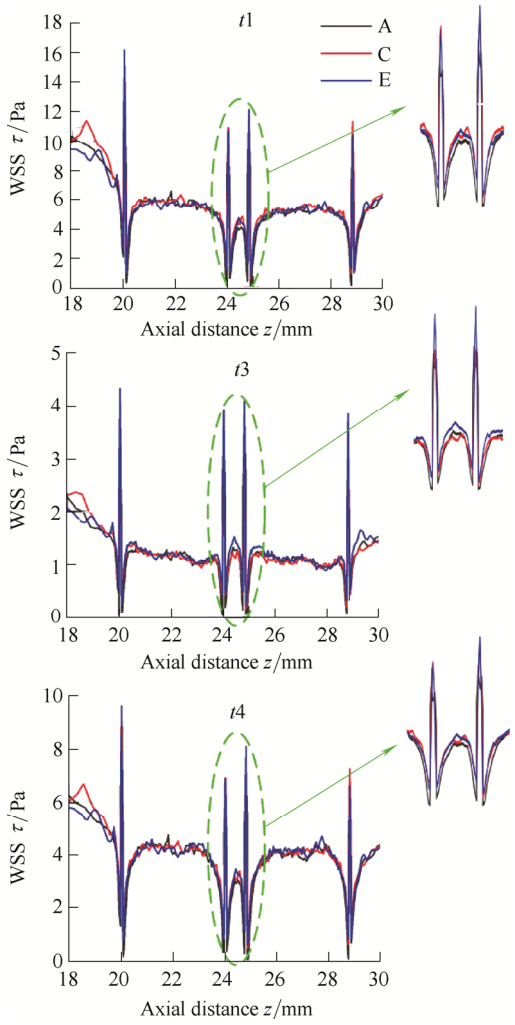

Fig. 10. Distributions of WSS for different strut cross-section

4 Discussion

These results clearly demonstrate that stent implantations greatly improve the blood flow field and strut cross-sections significantly influence the hemodynamics in stented arteries. As shown in Fig. 5, the models with different cross-section have different growth rates of the velocity near wall which would cause different degrees of flow disturbance. For the models with different strut width (e.g., A and B, C and D, E and F), the results of the velocity changes near wall are as follows: A<B, C<D, E<F. In combination with the previous studies[22–23] about the influence of strut height on hemodynamics, the AR of strut cross-section is considered as a decisive factor affecting the hemodynamics. Especially, the differences of the velocity values for Model E and F are largest among three groups, mainly because the changes of cross-sectional shapes are the most severe, as shown in Fig. 11. The largest velocity differences induced by stents with elliptical arc cross-section (Model E and F) demonstrate that the streamlines of strut cross-section is also a key factor affecting the hemodynamics. It is consistent with the result that stents with more streamlined cross-section exhibit better hemodynamics[22].

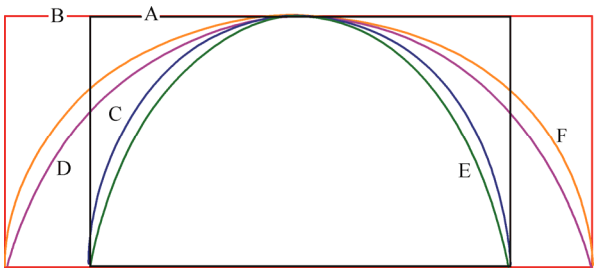

Fig. 11. Amplifier schematic of strut cross-sectional shape of stents for physical models

The differences of the velocity distributions in lines of L1–L8 are clearly displayed in Fig. 6 for the same model. The velocity difference of 0.1 m/s among these lines can be observed. It is mainly caused by the positions of lines in the stented segment. Obviously, in some regions with larger strut spacing of L2 and L3, L6 and L7, the velocity changes are significantly bigger than that with a relatively small strut spacing of L4 and L5. It is benefit to blood flow in some places with larger strut spacing which is in good agreement with the previous studies[19–20, 28]. Though strut spacing is not considered in this paper, it is still an important factor affecting the hemodynamics. It can also be validated that larger low-WSS areas are observed in places with small strut spacing as shown in Fig. 7. Therefore, the proper strut spacing is one of the best solutions for improving the hemodynamics of stents only when stents can be ensured to prevent plaque prolapse. As in the previous study[9], flow disturbance of stent downstream have been detected larger than that of stent upstream. It is possible that restenosis easily appear in the stent downstream regions.

The presence of low-WSS in stented regions might contribute to endothelial damage and restenosis development. As shown in Fig. 7, Fig. 8 and Table 2, the comparisons of the models with same AR on low-WSS area can be concluded as follows: A>E>C, B>F>D. Obviously, the influence of non-streamlined cross-section on low-WSS area is greater than that of the streamlined cross-section. Strut cross-sectional shape is a significant factor affecting the area of the low-WSS. Simultaneously, the area comparisons of the low-WSS for the models with similar cross-sectional shape, different AR can be concluded as follows: A>B, C>D, E>F. It also indicates that strut cross-sections with larger AR can cause smaller low-WSS area. The above results all show that stents with

streamlined cross-sections and a larger AR are more beneficial to blood flow, which is consistent with the previous results[23].

The inlet velocity is 0.2 m/s at the time of *t*2 and *t*5 during the cardiac cycle period which is equal to the inlet velocity of steady flow. The WSS distributions in *t*2 and *t*5 are employed to compare with that under steady flow. The result comparisons are shown in Fig. 12. It is obvious that the temporal WSS at the distal of the systole (*t*2) are lower than that at the distal of the diastole (*t*5). But it is difficult to compare qualitatively with the WSS distributions between steady and pulsatile flow. It can be computed for the percentage of low-WSS in *t*2 and *t*5 separately for quantitative comparisons. And the results related to WSS are depicted in Table 3.

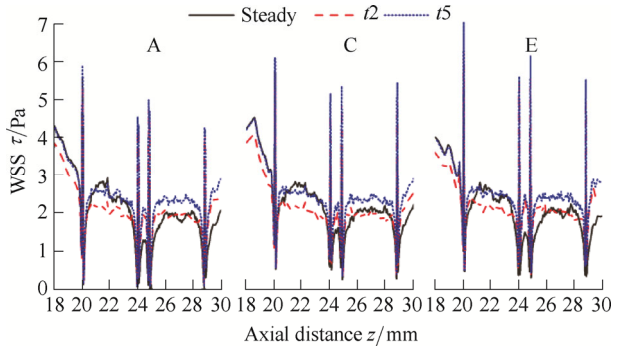

Fig. 12. Comparisons of WSS under steady and unsteady flow conditions with a same magnitude of inlet velocity for 0.2 m/s

Table 3. Comparison of main results for a same inlet velocity under different time points

Models & time points	The largest value of WSS τ_{max}/Pa	Area percentage of WSS <0.5 Pa p_{area}/%	Average WSS $\bar{\tau}$ /Pa
A & *t*2	6.10	3.40	2.690
A & *t*5	6.51	2.33	2.885
C & *t*2	6.39	0.16	2.700
C & *t*5	6.96	0.09	2.901
E & *t*2	7.45	0.19	2.712
E & *t*5	7.93	0.14	2.907

Under pulsatile conditions, the area percentage of low-WSS at *t*2 is higher than that of *t*5 for all models. The pulsatile calculated results show that the influence of cross-section on WSS is similar to that of the steady condition. It is still the largest for the influence of Model A on WSS, the following behind for Model E and the least for Model C. For Model A, the area percentages of low-WSS at *t*2and *t*5 reduce by 38.5% and 57.8%, respectively when compared with that of steady flow. For Model C, the area percentages of low-WSS at *t*2 and *t*5 reduce by 46.7% and 70%, respectively when compared with that of steady flow. For Model E, the area percentages of low-WSS at *t*2 and *t*5 reduce by 80.6% and 85.7%, respectively when compared with that of steady flow. By comparing quantitatively the results about the area percentage of the low-WSS, it is concluded that simulations of steady flow overestimate the area of low-WSS, which can lead to overestimate the risk of restenosis.

Hemodynamics is only part of the success of stent implantation. This study analyzes how stents with different cross-section alter the hemodynamics in the acute stage after stent implantations. It is no consideration to the appearance of thrombus which can occur within minutes to hours after stent implantation. It is well-known that the low-WSS regions can delay restoration of endothelial cells and increase the likelihood of restenosis, so it's important to optimize stent designs using CFD method to minimize flow disturbances. The size of low-WSS regions varies with the shapes and AR of strut cross-section. A better design of strut cross-section is to look for a proper streamline and the AR of strut cross-section for decreasing disturbed flow associated with platelet activation and accumulation.

The proposed physical models are based on simplified ideal status between the stents and the arteries, and the coronary artery is only assumed to be a straight single-layer vessel wall. The simplified assumptions may affect the simulation results. In order to more accurately estimate the simulation results, there are still some factors which need to be added into the current models, including the three-layer properties of vessel wall, the actual vessel status after stent implantation, the vessel models (curved and bifurcation models), and the compliance match between stents and arteries. Except for the mentioned parts, the fluid-structure interaction (FSI) method[33–34] also should be employed to study the interaction between blood and the arterial wall for a more precise analysis. Even so, the present simplified models still demonstrate the importance of the strut cross-sectional design on hemodynamics and provide some design ideas of stent structures.

5 Conclusions

Blood flow behaviors after implanting different stents are well investigated using the three-dimensional numerical simulation method. The strut cross-section of stents inevitably influences the hemodynamics of the stented segments which would be closely related to the restenosis process. Different results of the hemodynamics were significantly observed through changing the shapes and AR of the stent strut cross-section in the stented arteries. Based on the above results, the main conclusions are as follows.

(1) The flow performances of stents with streamlined cross-section for elliptical arc and circular arc are obviously superior to that of stents with non-streamlined cross-section for rectangle. So, it is beneficial to reduce the in-stent restenosis by the improvement in the shapes of stent strut cross-section in stent designs.

(2) Except for the shapes of stent strut cross-section, the AR of strut cross-section is also an important factor in stent designs. It will be more beneficial to improve the blood flow and reduce the restenosis for stents with a larger AR

cross-section.

(3) It would greatly reduce the disturbed flow by improving the cross-sectional parameters of stents. These results may guide stent designs and assist the clinician in selecting an appropriate stent for treating special lesions.

Although stents with more streamlined cross-section would be limited by present manufacturing technology. With the development of manufacturing technology, solid models of vessels and stents can be manufactured and experiments in vitro can be carried out for further studies.

References

[1] FRANK A O, WALSH P W, MOORE J E, Computational fluid dynamics and stent design[J]. *Artificial Organs*, 2002, 26(7): 614–621.

[2] SHEN X, YI H, NI Z, et al. Optimization of coronary stent structure design for maximizing the anti-compression mechanical property[J]. *Chinese Journal of Mechanical Engineering*, 2008, 21(6): 98–102.

[3] ETAVE F, FINET G, BOIVIN M, et al. Mechanical properties of coronary stents determined by using finite element analysis[J]. *Journal of Biomechanics*, 2001, 34(8): 1065–1075.

[4] MOORE J E, XU C P, GLAGOV S, et al. Fluid wall shear stress measurements in a model of the human abdominal aorta: oscillatory behavior and relationship to atherosclerosis[J]. *Atherosclerosis*, 1994, 110(2): 225–240.

[5] HE X J, KU D N. Pulsatile flow in the human left coronary artery bifurcation: Average conditions[J]. *Journal of Biomechanical Engineering-Transactions of the ASME*, 1996, 118(1): 74–82.

[6] TOMINAGA R, KAMBIC H E, EMOTO H, et al. Effect of design geometry of intravascular endoprotheses on stenosis rate in normal rabbits[J]. *American Heart Journal*, 1992, 123(1): 21–28.

[7] ROGERS C, EDELMAN E R. Endovascular stent design dictates experimental restenosis and thrombosis[J]. *Circulation*, 1995, 91(12): 2995–3001.

[8] GARASIC J M, EDELMAN E R, SQUIRE J C, et al. Stent and artery geometry determine intimal thickening independent of arterial injury[J]. *Circulation*, 2000, 101(7): 812–818.

[9] PEACOCK J, HANKINS S, JONES T, et al. Flow instabilities induced by coronary-artery stents: assessment with an in-Vitro pulse duplicator[J]. *Journal of Biomechanics*, 1995, 28(1):17–26.

[10] LADISA J F, OLSON L E, MOLTHEN R C, et al. Alterations in wall shear stress predict sites of neointimal hyperplasia after stent implantation in rabbit iliac arteries[J]. *American Journal of Physiology-Heart and Circulatory Physiology*, 2005, 288(5): H2465–H2475.

[11] KASTRATI A, MEHILLI J, DIRSCHINGER J, et al. Restenosis after coronary placement of various stent types[J]. *American Journal of Cardiology*, 2001, 87(1): 34–39.

[12] WENTZEL J J, KRAMS R, SCHUURBIERS J C H, et al. Relationship between neointimal thickness and shear stress after wallstent implantation in human coronary arteries[J]. *Circulation*, 2001, 103(13): 1740–1745.

[13] KASTRATI A, MEHILLI J, DIRSCHINGER J, et al. Intracoronary stenting and angiographic results: Strut thickness effect on restenosis outcome (ISAR-STEREO) trial[J]. *Circulation*, 2001, 103(23): 2816–2821.

[14] PANT S, BRESSLOFF N W, FORRESTER A I J, et al. The influence of strut-connectors in stented vessels: A comparison of pulsatile flow through five coronary stents[J]. *Annals of Biomedical Engineering*, 2010, 38(5): 1893–1907.

[15] VERDONCK P. The role of computational fluid dynamics for artificial organ design[J]. *Artificial Organs*, 2002, 26(7): 569–570.

[16] KRUEGER U, ZANOW J, SCHOLZ H. Computational fluid dynamics and vascular access[J]. *Artificial Organs*, 2002, 26(7): 571–575.

[17] LEE C-J, UEMIYA N, ISHIHARA S, et al. A comparison of estimation methods for computational fluid dynamics outflow boundary conditions using patient-specific carotid artery[J]. *Proceedings of the Institution of Mechanical Engineers Part H-Journal of Engineering in Medicine*, 2013, 227(H6): 663–671.

[18] AZAOUZI M, MAKRADI A, BELOUETTAR S. Numerical investigations of the structural behavior of a balloon expandable stent design using finite element method[J]. *Computational Materials Science*, 2013, 72(0): 54–61.

[19] BERRY J L, SANTAMARINA A, MOORE J E, et al. Experimental and computational flow evaluation of coronary stents[J]. *Annals of Biomedical Engineering*, 2000, 28(4): 386–398.

[20] LADISA J F, OLSON L E, GULER I, et al. Stent design properties and deployment ratio influence indexes of wall shear stress: a three-dimensional computational fluid dynamics investigation within a normal artery[J]. *Journal of Applied Physiology*, 2004, 97(1): 424–430.

[21] MORTON A C, CROSSMAN D, GUNN J, The influence of physical stent parameters upon restenosis[J]. *PathologieBiologie*, 2004, 52(4): 196–205.

[22] MEJIA J, RUZZEH B, MONGRAIN R, et al. Evaluation of the effect of stent strut profile on shear stress distribution using statistical moments[J]. *Biomedical Engineering Online*, 2009, 8: 8.

[23] JIMENEZ J M, DAVIES P F. Hemodynamically driven stent strut design[J]. *Annals of Biomedical Engineering*, 2009, 37(8): 1483–1494.

[24] BARAKAT A I, CHENG E T. Numerical simulation of fluid mechanical disturbance induced by intravascular stents[C/CD]. *International Conference on Mechanics in Medicine and Biology*, 2000.

[25] CHOI H W, BARAKAT A I. Numerical study of the impact of non-Newtonian blood behavior on flow over a two-dimensional backward facing step[J]. *Biorheology*, 2005, 42(6): 493–509.

[26] JUNG J W, LYCZKOWSKI R W, PANCHAL C B, et al. Multiphase hemodynamic simulation of pulsatile flow in a coronary artery[J]. *Journal of Biomechanics*, 2006, 39(11): 2064–2073.

[27] DWYER H A, CHEER A Y, RUTAGANIRA T, et al. Calculation of unsteady flows in curved pipes[J]. *Journal of Fluids Engineering-Transactions of the ASME*, 2001, 123(4): 869–877.

[28] DEHLAGHI V, SHADPOOR M T, NAJARIAN S. Analysis of wall shear stress in stented coronary artery using 3D computational fluid dynamics modeling[J]. *Journal of Materials Processing Technology*, 2008, 197(1–3): 174–181.

[29] LADISA J F, GULER I, OLSON L E, et al. Three-dimensional computational fluid dynamics modeling of alterations in coronary wall shear stress produced by stent implantation[J]. *Annals of Biomedical Engineering*, 2003, 31(8): 972–980.

[30] BALOSSINO R, GERVASO F, MIGHAVACCA F, et al. Effects of different stent designs on local hemodynamics in stented arteries[J]. *Journal of Biomechanics*, 2008, 41(5): 1053–1061.

[31] MALEK A M, ALPER S L, IZUMO S. Hemodynamic shear stress and its role in atherosclerosis[J]. *JAMA-Journal of the American Medical Association*, 1999, 282(21): 2035–2042.

[32] RENEMAN R S, ARTS T, HOEKS A P G. Wall shear stress - an important determinant of endothelial cell function and structure - in the arterial system in vivo[J]. *Journal of Vascular Research*, 2006, 43(3): 251–269.

[33] MALVE M, PEREZ DEL PALOMAR A, CHANDRA S, et al. FSI analysis of a human Trachea before and after prosthesis implantation[J]. *Journal of Biomechanical Engineering-Transactions of the ASME*, 2011, 133(7).

[34] KARIMI A, NAVIDBAKHSH M, RAZAGHI R, et al. A computational fluid-structure interaction model for plaque vulnerability assessment in atherosclerotic human coronary arteries[J]. *Journal of Applied Physics*, 2014, 115(14).

Biographical notes

JIANG Yongfei, born in 1979, is currently a PhD candidate at *State Key Laboratory for Manufacturing Systems Engineering, Xi'an Jiaotong University, China*. She received her master degree on mechatronics from *Chang'an University, China*, in 2008. Her research interests include the hemodynamics after stent implantation and stent structural design.
Tel: +86-29-83399005; E-mail: jyfpp@126.com

ZHANG Jun, born in 1978, is currently an associate professor at *State Key Laboratory for Manufacturing System Engineering, Xi'an Jiaotong University, China. He* received his PhD degree from *Xi'an Jiaotong University, China*, in 2009. His research interest includes high-speed machining.

ZHAO Wanhua, born in 1965, is currently a professor, a PhD candidate supervisor and a chair professor of "Cheung Kong Scholar" at *State Key Laboratory for Manufacturing System Engineering, Xi'an Jiaotong University, China*.
Tel: +86-29-83399520; E-mail: whzhao@mail.xjtu.edu.cn